RMIT
UNIVERSITY

Thank you for downloading this document from the RMIT Research Repository.

The RMIT Research Repository is an open access database showcasing the research outputs of RMIT University researchers.

RMIT Research Repository: http://researchbank.rmit.edu.au/

See this record in the RMIT Research Repository at:

http://researchbank.rmit.edu.au/view/rmit:21951

Version: Published Version

Link to Published Version:

http://dx.doi.org/10.1088/1367-2630/13/4/045015

PLEASE DO NOT REMOVE THIS PAGE

Engineering chromium-related single photon emitters in single crystal diamonds

I Aharonovich, S Castelletto, B C Johnson, J C McCallum and S Prawer

School of Physics, University of Melbourne, Parkville, Victoria 3010, Australia
E-mail: i.aharonovich@pgrad.unimelb.edu.au

Abstract. Color centers in diamond, as single photon emitters, are leading candidates for future quantum devices due to their room temperature operation and photostability. The recently discovered chromium-related centers are particularly attractive because they possess narrow bandwidth emission and a very short lifetime. In this paper, we investigate the fabrication methodologies for engineering these centers in monolithic diamond. We show that the emitters can be successfully fabricated by ion implantation of chromium in conjunction with oxygen or sulfur. Furthermore, our results indicate that the background nitrogen concentration is an important parameter, which governs the probability of success in generating these centers.

Developing novel solid state systems that can generate single photons on demand at room temperature is a prime goal in the quantum information science community [1, 2]. Impurities in diamond offer a unique advantage over other systems as some of them are optically active and can be employed as true single photon sources [3]. The nitrogen vacancy (NV) center, for example [4], has been the subject of intense research [4]–[7], particularly due to its optical spin readout capabilities and its potential use as a high-sensitivity magnetic sensor [8, 9]. However, the optical properties of this center are limited by a strong phonon coupling, resulting in broad emission (~ 100 nm) of which only 4% is concentrated in the zero phonon line (ZPL). This is a significant drawback for many quantum optical applications including quantum key distribution, quantum metrology and optical quantum computation.

Alternative centers with narrower emission lines that are also more suitable for microcavity integration are required. Nickel- and silicon-related emitters have been studied as plausible candidates because some of the centers show narrow emission lines in the near infrared (NIR) [10]–[13]. However, nickel centers such as NE8 are difficult to fabricate due to the requirement of four nitrogen atoms to form a complex with the Ni impurity. Until recently the silicon vacancy (SiV) has not been considered as a good candidate for single defect devices due to a very high nonradiative decay term, limiting its quantum efficiency to only 5% [14]. Surprisingly, however, the recent fabrication of SiV in chemical vapor deposition (CVD)-grown nanodiamonds formed on an iridium substrate demonstrated outstanding and unexpected brightness and spectral properties [15]. These improvements are likely to spur substantial research into the photophysics of the SiV center, in particular, fabricating centers with similar brightness in monolithic diamond by ion implantation.

Recently, a new class of single photon emitters associated with chromium impurities in diamond [16]–[18] was discovered. These centers show bright fluorescence in the NIR and possess a short radiative lifetime. Moreover, the linear transition dipole both in absorption and in emission [19] is considered ideal for three-dimensional orientation imaging and tracking with various microscopy methods [20]–[22].

The chromium emitters were originally discovered during diamond growth on a sapphire substrate. The Cr atoms that are present in the sapphire substrate were incorporated into the growing crystal through gas phase diffusion [10]. However, to achieve the best intrinsic photo-physical properties of optical centers, such as reduced inhomogeneous broadening and Fourier transform-limited emission [23], emitters should be fabricated into single crystal diamonds [24]. Therefore, methods for creating optical centers with high efficiency in bulk material are of paramount importance for quantum optical devices [25, 26]. Furthermore, for scalable quantum device architectures and for integration with other optical structures, accurate positioning and a high formation probability are required. These conditions have not yet been fulfilled for the particular case of chromium centers. Above all, the role of other impurities in the formation of the center remains poorly understood. A formation study of this center by conventional ion implantation techniques is also required in order to assess the possible deterministic fabrication pathways to engineer the centers in nanodiamonds sized below 50 nm. This would have immediate applications in bio-sensing.

In this paper, we investigate the role of co-dopants, such as nitrogen and oxygen, in the formation of chromium centers in diamond by ion implantation techniques. We perform a range of co-implantations of various impurities together with Cr ions, to determine their effect on the formation of single emitters [17]. We also consider the target material and show that the background nitrogen level present natively inside the diamond is a crucial parameter. Our present studies aim to provide a sound basis for further research into the fabrication of chromium emitters and to gather important information regarding their atomistic structure. We envisage that the results will encourage further experiments aimed to improve the formation yield of the centers up to the desired level necessary for implementing deterministic devices based on Cr single emitters in diamond [25].

The ion implantation of chromium, oxygen, silicon, boron, nitrogen and sulfur was performed with a National Electrostatics Corporation 150 kV low-energy ion implanter at the Australian National University. During implantation the single crystal diamond samples ($3 \times 3 \times 0.5$ mm^3) were affixed to a temperature-controllable nickel block with clamps. All implantations were performed at room temperature in ultra-high-vacuum conditions

Table 1. Implanted elements and the corresponding implantation energies and projected ranges.

Element	Implantation energy (keV)	Projected range (nm)
Chromium	50	25 ± 7
Oxygen	19.5	25 ± 8
Silicon	34	25 ± 7
Boron	13	25 ± 8
Sulfur	38	25 ± 7
Nitrogen	18	25 ± 8
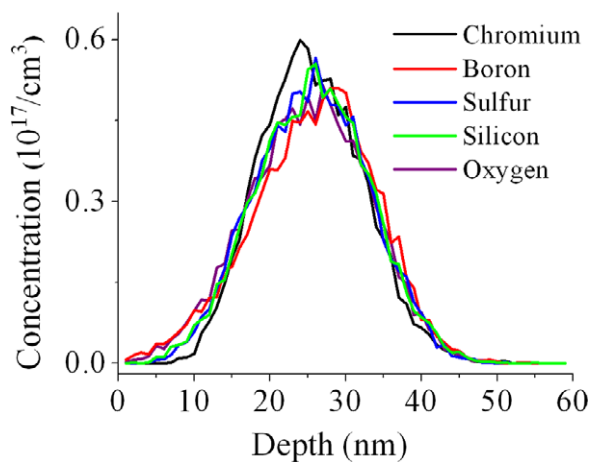
Figure 1. SRIM simulation of the concentration profiles of the implanted ions.

($\sim 10^{-7}$ torr). The implantation ion energies for chromium and the co-implanted species were all chosen to result in a projected range of 25 nm and are listed in table 1. This allows efficient detection of the light emitted from the centers. Figure 1 shows the concentration profiles of the implanted ions as determined with the Monte Carlo simulation code Stopping and Range of Ions in Matter (SRIM; http://www.SRIM.org).

After implantation, the samples were annealed at 1000 °C in a forming gas ambient (95% Ar–5% H_2) for 2 h. This is a typical procedure to induce vacancy diffusion in diamond and to repair damage caused by the implantation. Note that the annealing step applied after the implantation is not sufficient to cause any diffusion of the implanted atoms (Cr, Si, B, O and N) in the diamond lattice [27]–[30].

The samples were then optically characterized to identify chromium-related single emitters. This was performed using a home-built confocal microscope with a Hanbury Brown and Twiss (HBT) setup to gain information regarding the photon statistics of the centers. A fiber-coupled continuous wave diode laser emitting at 682 nm was used for excitation. The diamond sample was mounted on a piezo *XYZ* stage with 0.2 nm resolution, allowing $100 \times 100 \, \mu m^2$ scans. The emitted light was collected using a high numerical aperture objective (NA = 0.9) and coupled to a 62.5 μm core multimode fiber, which acts as an aperture. A 50:50 fiber-coupled beam splitter guided the photons to two single photon counting detectors (APDs) and their

Table 2. Summary of chromium-related ion implantations into type IIA CVD ([N]< 1 ppm, [B]< 0.05 ppm) diamond. Yield is the number of single chromium emitters per implanted chromium ion.

Diamond material	Fluences (ions cm^{-2})	Sample no.	Yield (%)	Density of Cr centers (centers cm^{-2})
	1×10^{11} Cr + 1×10^{11} Si	(1)	10^{-5}	10^4
	1×10^{13} Cr + 1×10^{13} Si	(2)	10^{-7}	10^4
	1×10^{11} Cr	(3)	10^{-5}	10^4
	1×10^{13} Cr	(4)	10^{-7}	10^4
	1×10^{10} Cr + 1.5×10^{10} O	(5)	10^{-3}	10^5
Type IIA	2×10^{10} Cr + 3×10^{10} O	(6)	5×10^{-4}	10^5
[N] < 1 ppm	1×10^{11} Cr + 1.5×10^{11} O	(7)	10^{-4}	10^5
[B] < 0.05 ppm	1×10^{11} Cr + 5×10^{11} O	(8)	10^{-4}	10^5
	1×10^{11} Cr + 2×10^{12} O	(9)	10^{-4}	10^5
	1×10^{12} Cr + 1.5×10^{12}O	(10)	10^{-5}	10^5
	1×10^{13} Cr + 1.5×10^{13} O	(11)	10^{-7}	10^4
	1×10^{11} Cr + 3×10^{11} S	(12)	10^{-4}	10^4
	1×10^{11} Cr + 1×10^{11} B	(13)	10^{-5}	10^4
	1×10^{11} Cr + 1×10^{12} B	(14)	10^{-5}	10^4

outputs were sent to the start and stop inputs of a time correlator card. All the measurements were carried out at room temperature. Spectroscopy has been performed to determine the typical Cr emission lines associated with a particular bright spot on the confocal map.

We first investigated the co-implantation of chromium with oxygen into type IIA CVD ([N]< 1 ppm, [B]< 0.05 ppm) samples. This was motivated by the fact that implantation of oxygen into silicon increased the proportion of Er that was present in the optically active Er^{3+} state [31]–[33]. Although Cr and Er might appear chemically equivalent (incorporation into lattice in 3+ charge state), their diffusivity, the nature of electronic transitions (3d versus 4f) and their susceptibility to crystal fields are quite different, which may influence the formation rate of chromium centers in diamond.

Our experiments based on co-implantation of chromium and oxygen or select other species (Si, S and B) into diamond are summarized in table 2. Figure 2 shows the main experimental results graphically. The yield is calculated by dividing the density of the observed centers by the chromium ion fluence and is given in units of %.

Figures 3(a) and (b) show typical confocal maps recorded from samples 3 and 7, respectively. It is clearly seen that more bright centers can be found on sample 7, which was co-implanted with oxygen, rather than sample 3, which was implanted with chromium only.

Figure 4(a) shows a typical spectrum of the chromium-related center. The inset represents the anti-bunching measurement recorded from the same emitter employing the HBT setup, demonstrating that the center is a single photon emitter. Narrow bandwidth lines with full-width at half-maximum (FWHM) ∼4 nm were routinely observed from the chromium-implanted samples. The histogram of the ZPLs is shown in figure 4(b). Similar ZPLs were observed in samples 1–14. The large distribution of ZPLs is most likely due to different local charge densities in the proximity of each emitter.
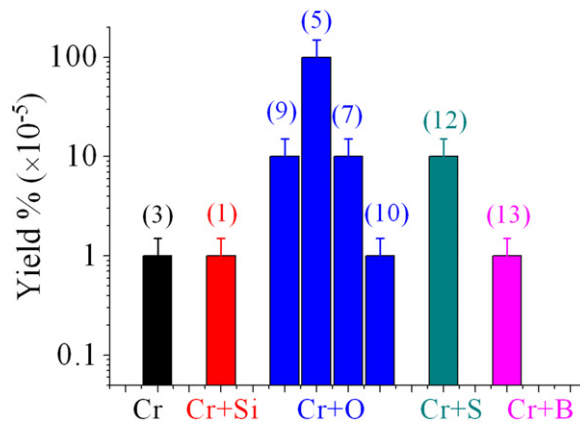
Figure 2. Various implantation routes employed to investigate the formation of Cr-related centers in type IIA CVD ([N]< 1ppm, [B]< 0.05 ppm) diamond. The number in brackets denotes the sample number, as shown in table 2. Yield is the number of single chromium emitters per implanted chromium ion.
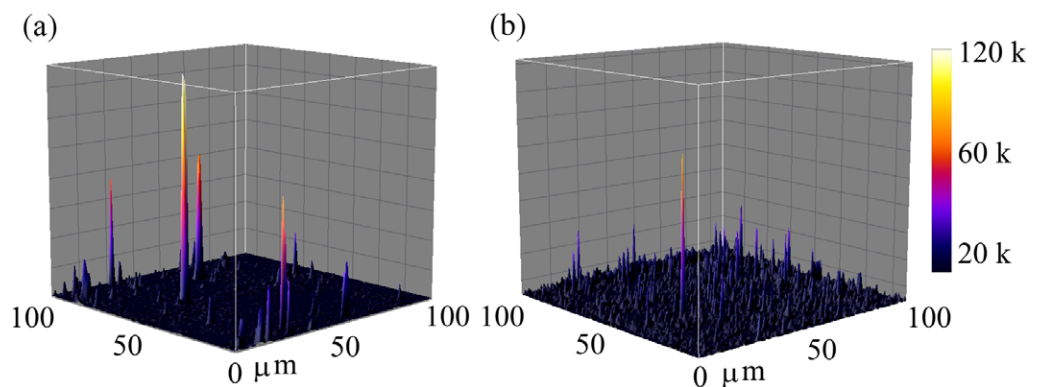

Figure 3. Confocal map recorded from a diamond sample implanted with (a) chromium and oxygen (sample 7) and (b) chromium only (sample 3). More single emitters are clearly observed at sample 7, which had chromium co-implanted with oxygen.

In our earlier work on chromium-related emitters in CVD-grown nanodiamonds [16], the emitters are formed through diffusion from the growth substrate and possess different properties (e.g. a two-level system rather than a three-level). The incorporated atoms have enough energy to diffuse and occupy the most stable atomic site within the nanodiamond crystal. In the present work, the emitters are engineered in a bulk crystal by ion implantation. Ion implantation results in an arbitrary position of the implanted atom, and the annealing sequence only heals the implantation damage but does not cause any diffusion of the atoms. This may explain the variation of wavelengths in the implanted samples.

Implantation of 1×10^{11} Cr cm^{-2} into type IIA CVD diamond (sample 3) yields on average 1 optically active Cr center per $100 \times 100\,\mu m^2$ scan. This indicates a rather low conversion probability of implanted Cr into optically active defects. Increasing the Cr fluence by two orders of magnitude decreases the yield by two orders of magnitude (samples 3 and 4).
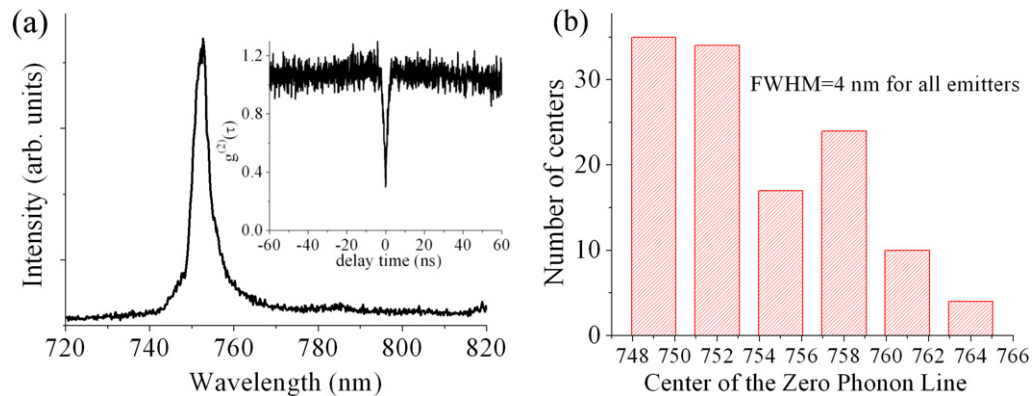
Figure 4. (a) PL spectrum of a chromium-related emitter. The inset represents the $g^{(2)}(\tau)$ function recorded from the same emitter demonstrating that the addressed center is a single photon emitter. (b) Histogram of the ZPLs of chromium-related emitters found in different samples.

This may indicate that residual implantation damage plays a role in limiting the yield of the centers. The increased damage at higher fluences could further reduce the impurity diffusivities [30] and/or reduce the probability of impurities attaining the required charge state. Co-implantation of Cr and O increases the yield by an order of magnitude or more (samples 5–9), but again an increased fluence results in a reduced yield. The highest yield was obtained for $1 \times 10^{10}\,\mathrm{Cr} + 1.5 \times 10^{10}\,\mathrm{O}$ ions cm^{-2} (sample 5). It is important to note that the chromium centers were repeatedly fabricated in type IIA CVD ([N]< 1 ppm, [B]< 0.05 ppm) diamond but could not be formed in other types of diamond substrates as discussed further below.

Both oxygen and sulfur increase the yield of optically active Cr centers (samples 5–12). The ratio of chromium-related single emitters observed in the co-implantation of chromium and oxygen/sulfur to those in other implantations was as high as $10:1$. Since sulfur and oxygen are located in the same column in the periodic table, they are expected to behave similarly when introduced into the diamond lattice. Sulfur defects in diamond have been investigated as potential donors to achieve n-type material. It is assumed that sulfur occupies a substitutional lattice site in diamond [28]. Theoretical work also predicts that oxygen will occupy a substitutional lattice site.

The general low formation probability of all implantation schedules studied is consistent with an expectation that the Cr and oxygen (or sulfur) atoms must be in very close proximity following the implantation process for the appropriate optically active charge state to form during the subsequent annealing, especially because the diffusivities are expected to be very low in the annealing regime used.

As noted earlier, the role of oxygen and sulfur in the formation of optically active Cr centers in diamond may be similar to the role O plays in Er doping of silicon. In silicon, under the processing conditions used, the diffusivity of oxygen is high enough that oxygen present in the silicon bulk can combine with a proportion of the implanted Er to form the optically active center. Co-implantation of erbium and oxygen into silicon greatly enhances the Er^{3+} emission [31]–[33]. Extended x-ray absorption fine structure measurements on Er- and O-doped silicon have shown that Er is coordinated by four to six O atoms [31]. Direct bonding is therefore important in forming the optically active center in this system.

Co-implantation of silicon and chromium was performed to test the damage effect associated with the implantation. Furthermore, silicon has a similar electronic configuration as carbon and hence is not a donor or an acceptor in diamond. Si will only produce damage and introduce more vacancies. This implantation procedure followed by the standard annealing treatment did not enhance the number of Cr centers compared to the co-implantation of Cr and O (samples 1 and 7). These results confirm that the role of oxygen/sulfur is related to a charge transfer rather than assisting in the generation of vacancies.

To investigate the effect of p-doping, chromium and boron were co-implanted (samples 13 and 14). CrB pairs are speculated to be responsible for some optically active centers in silicon when Cr is present; therefore, there is scientific interest in investigating this pair in diamond [35, 36]. The results of these implants showed that only a limited number of chromium emitters were formed, similar to the chromium only or chromium plus silicon co-implantation schedules. When no donor is co-implanted, the charge state configuration could be aided by as-grown impurities (e.g. from nitrogen). However, as was shown experimentally, the probability of forming the chromium emitters is significantly reduced.

Surprisingly, for the samples implanted with 1×10^{11} Cr cm^{-2} no significant oxygen fluence dependence was observed. We varied the Cr : O ratio from 1 : 1.5 to 1 : 20 (samples 7 and 9); however, we did not observe any dependence on the formation probability of the centers or their optical properties. The optical properties of the centers were likewise unaffected by the greater oxygen concentration. To unambiguously prove the involvement of the donor, low densities of Cr should be implanted ($< 1 \times 10^{10}$ Cr cm^{-2}). Such studies are planned and the results will be reported when available.

Such an experiment would also explain the lack of scalability of the observed centers with the chromium fluence. Comparing samples 5, 7 and 10, the number of active emitters did not increase although the chromium fluence was increased by three orders of magnitude. This may indicate that a fluence of 1×10^{11} Cr cm^{-2} is approaching saturation for converting an implanted ion into an optical center.

In the second part of this work, we investigated the dependence of the target diamond material on Cr center formation. Three types of diamond were compared: CVD single crystal type IIA diamond ([N]$<$ 1 ppm, [B]$<$ 0.05ppm), ultra-pure CVD single crystal diamond ([N]$<$ 5 ppb, [B]$<$ 1 ppb), both purchased from Element Six, and a type IB sample ([N]$<$ 100 ppm, [B]$<$ 0.1 ppm) produced by Sumitomo. This last crystal was cut and polished from a large single crystal, which was synthesized under high-pressure high-temperature (HPHT) conditions. Table 3 summarizes the performed experiments. The annealing sequence was the same as that described above.

The results of this section are intriguing. When the implantation sequence that generated single emitters in type IIA diamond (e.g. 1×10^{11} Cr $+ 1.5 \times 10^{11}$ O) was applied to an ultra-pure or a type Ib diamond, single chromium-related centers were never observed (samples 15–18 and 21–25). Figure 5 shows a photoluminescence (PL) spectrum recorded from the ultra-pure diamond sample (sample 15). A broad emission is observed, similar to the Cr-related cathodoluminescence map reported in [37]. Neither narrow bandwidth emission nor single photon characteristics were observed from this sample.

The main difference between these diamonds is the amount of nitrogen. While in an ultra-pure sample, the level of nitrogen is extremely low, less than ppb, in type Ib the concentration of nitrogen is extremely high ($\sim$100 ppm). It is therefore likely that nitrogen plays a crucial role in the formation of the centers. It was shown recently that in an ultra-pure material, there is a

Table 3. Various implantation routes employed to investigate the formation of Cr-related centers in an ultra-pure CVD diamond ([N]< 5 ppb, [B]< 1 ppb) and in a type Ib diamond ([N]< 100 ppm, [B]< 0.1 ppm) grown by the HPHT method.

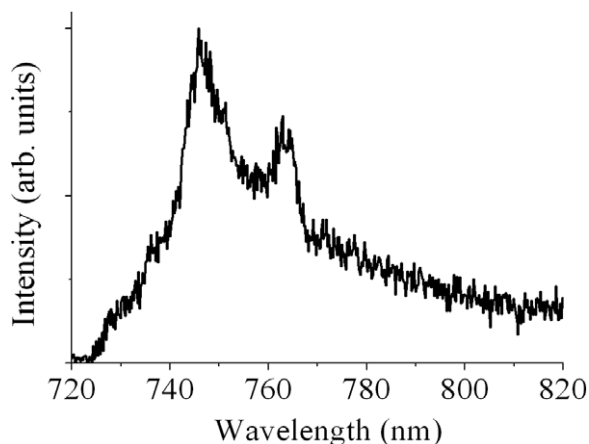| Diamond type	Implantation details	Sample no.	Comments
Ultra-pure	1×10^{11} Cr + 1.5×10^{11} O	15	
[N] < 5 ppb	2×10^{11} Cr + 3×10^{11} O	16	
[B] < 1 ppb	2×10^{10} Cr	17	No single centers or
	2×10^{10} Cr + 2×10^{10} B	18	narrow PL lines were
	1×10^{11} Cr + 1.5×10^{11}O + 1×10^{9}N	19	found at all
	1×10^{11} Cr + 1.5×10^{11} O + 1×10^{11} N	20	
Type Ib	1×10^{11} Cr + 1×10^{11} Si	21	
[N] < 100 ppm	1×10^{13} Cr + 1×10^{13} Si	22	No single centers or
[B] < 0.1 ppm	1×10^{11} Cr	23	narrow PL lines were
	1×10^{13} Cr	24	found at all
	1×10^{11} Cr + 1.5×10^{11} O	25	
	1×10^{13} Cr + 1.5×10^{13} O	26	

Figure 5. PL spectrum recorded from chromium- and oxygen-implanted ultra-pure diamond.

large electron depletion layer [38], which may hinder the formation of the center in an ultra-pure material.

The influence of nitrogen is likely to dominate the charge state of the center. If its concentration is too high or too low, the chromium emitters may not be formed because the correct charge state cannot be achieved. Theoretical work by Gali *et al* [34] indicates that the charge state of substitutional oxygen depends very sensitively on the Fermi level, so this may also play a role. The O^{+2} state is stable when the Fermi level is in the range of 0–1.39 eV (measured relative to the top of the valence band), while the negatively charged oxygen, O^{-}, will be stable if the Fermi level is above 2.89 eV. Such strong dependence on the Fermi level

means that the oxygen located at a vacancy position in diamond has very much amphoteric character and thus can act as an electron trap in diamond.

To investigate this hypothesis further, we performed two additional experiments: (i) we co-implanted nitrogen with chromium and oxygen (samples 19 and 20). For sample 20, the nitrogen fluence was chosen to match the ~ 1 ppm of native nitrogen available in type IIA diamonds. (ii) Sample 20 was annealed and re-implanted with chromium. This was done to achieve stabilization of the implanted nitrogen so that the nitrogen atoms can occupy the most stable location in the diamond lattice. However, even in this case no single centers or narrow PL lines were observed. This stresses the importance of having a particular initial nitrogen concentration in the target diamond sample. Note that only a small fraction of the implanted nitrogen atoms occupy substitutional lattice sites and form substitutional nitrogen defects. The rest will bond to a vacancy forming NV centers. Moreover, nitrogen–interstitial complexes can be produced in significant concentrations due to N implantation, and can act as electron traps and are stable even at temperatures where the NV center anneals out [39]. Full activation of the nitrogen will require higher annealing temperatures currently not available in our laboratory.

The lack of formation of chromium emitters in ultra-pure material, and the very weak dependence of the formation of chromium centers on the fluence of implanted chromium ions, leaves some open questions. We do stress that unimplanted samples or samples that were implanted with other ions (e.g. N, Ni or He) were scanned, but no narrow lines or single emitters in the same spectral window were ever observed. We cannot rule out the possibility that chromium activates some other impurities, available in type IIA diamond; however, this seems extremely unlikely since other materials are expected to do so as well.

In the last part of our experiments, we performed high-energy ion implantation of 9 MeV chromium and 5.1 MeV oxygen to fluences of 1×10^{11} and 1.5×10^{11} ion cm^{-2}, respectively, on an NEC 1.7MV tandem accelerator. After the same annealing sequence, the samples were investigated optically. The results of the deep implantation were similar to the shallow one, with an average yield of 10^{-4}%. This observation strongly suggests that vacancies are not a limiting factor in the formation of the center, because more than 5000 vacancies per ion are formed during the high-energy implantation. This is much greater than that produced by the low-energy implanted ions. On the other hand, it was shown recently that NV formation dramatically increases when nitrogen is implanted deep into the diamond. The higher the implantation energy, the more vacancies are created around the substitutional nitrogen atom, giving rise to a higher yield of NV centers [40]. Therefore, even if vacancies are not forming the chromium center, a more radical condition (such as a specific charge state or complex with additional impurity) must be met to form the centers.

To summarize, by employing ion implantation and confocal microscopy, we investigated the fabrication methodologies of chromium-related centers and the influence of co-implanted impurities. Our results provide a robust recipe for production of such centers in CVD type IIA single crystal diamond, despite their low formation probability. The best recipe for producing chromium single photon emitters is implanting chromium and either oxygen or sulfur to a fluence of $\sim 1 \times 10^{10}$ ions cm^{-2} followed by a 2 h, 1000 °C anneal in a forming gas ambient.

We acknowledge that some of the results may have various interpretations and peculiarities (e.g. the centers were never found in an ultra-pure material and there is no clear scalability with the implantation dose). However, we believe that the presented information is an important milestone toward a complete understanding of the emitters' structure.

IOP Institute of Physics ΦDEUTSCHE PHYSIKALISCHE GESELLSCHAFT

To further the progress in understanding the physical properties of the new family of chromium defects, further experimental and theoretical work is required [41]. In particular, implantation of Cr atoms with low doses and a thorough investigation of different annealing conditions should be considered [42]. Once solid theoretical support is provided, it may be possible to increase the fabrication yield of the centers and understand the atomic composition of the defects.

Acknowledgments

References

[1] Ladd T D, Jelezko F, Laflamme R, Nakamura Y, Monroe C and O'Brien J L 2010 Quantum computers *Nature* **464** 45–53

[2] O'Brien J L, Furusawa A and Vuckovic J 2009 Photonic quantum technologies *Nat. Photonics* **3** 687–95

[3] Greentree A D, Fairchild B A, Hossain F M and Prawer S 2008 Diamond integrated quantum photonics *Mater. Today* **11** 22–31

[4] Kurtsiefer C, Mayer S, Zarda P and Weinfurter H 2000 Stable solid-state source of single photons *Phys. Rev. Lett.* **85** 290–3

[5] Toyli D M, Weis C D, Fuchs G D, Schenkel T and Awschalom D D 2010 Chip-scale nanofabrication of single spins and spin arrays in diamond *Nano Lett.* **10** 3168–72

[6] Brouri R, Beveratos A, Poizat J P and Grangier P 2000 Photon antibunching in the fluorescence of individual color centers in diamond *Opt. Lett.* **25** 1294–6

[7] Rabeau J R, Reichart P, Tamanyan G, Jamieson D N, Prawer S, Jelezko F, Gaebel T, Popa I, Domhan M and Wrachtrup J 2006 Implantation of labelled single nitrogen vacancy centers in diamond using N-15 *Appl. Phys. Lett.* **88** 023113

[8] Maze J R *et al* 2008 Nanoscale magnetic sensing with an individual electronic spin in diamond *Nature* **455** 644–8

[9] Balasubramanian G *et al* 2008 Nanoscale imaging magnetometry with diamond spins under ambient conditions *Nature* **455** 648–52

[10] Aharonovich I, Zhou C Y, Stacey A, Treussart F, Roch J F and Prawer S 2008 Formation of color centers in nanodiamonds by plasma assisted diffusion of impurities from the growth substrate *Appl. Phys. Lett.* **93** 243112

[11] Gaebel T, Popa I, Gruber A, Domhan M, Jelezko F and Wrachtrup J 2004 Stable single-photon source in the near infrared *New J. Phys.* **6** 98–104

[12] Steinmetz D, Neu E, Meijer J, Bolse W and Becher C 2010 Single photon emitters based on Ni/Si related defects in single crystalline diamond *Appl. Phys.* B submitted arXiv:1007.0202

[13] Wu E, Jacques V, Zeng H P, Grangier P, Treussart F and Roch J F 2006 Narrow-band single-photon emission in the near infrared for quantum key distribution *Opt. Express* **14** 1296–303

[14] Wang C L, Kurtsiefer C, Weinfurter H and Burchard B 2006 Single photon emission from SiV centres in diamond produced by ion implantation *J. Phys. B: At. Mol. Opt. Phys.* **39** 37–41

[15] Neu E, Steinmetz D, Riedrich-Moeller J, Gsell S, Fischer M, Schreck M and Becher C 2011 Single photon emission from silicon-vacancy centres in chemical vapour deposition nano-diamonds on iridium *New J. Phys.* **13** 025012

[16] Aharonovich I, Castelletto S, Simpson D A, Stacey A, McCallum J, Greentree A D and Prawer S 2009 Two-level ultrabright single photon emission from diamond nanocrystals *Nano Lett.* **9** 3191–5

[17] Aharonovich I, Castelletto S, Simpson D A, Johnson B C, Stacey A, McCallum J, Greentree A D and Prawer S 2010 Chromium single-photon emitters in diamond fabricated by ion implantation *Phys. Rev.* B **81** 121201

[18] Aharonovich I, Castelletto S, Simpson D, Greentree A D and Prawer S 2010 Photophysics of chromium-related diamond single-photon emitters *Phys. Rev.* A 043813

[19] Aharonovich I, Castelletto S, Gibson B C, Johnson B C and Prawer S 2010 Imaging and quantum efficiency measurement of chromium emitters in diamond *Phys. Rev. Lett.* **105** 217403

[20] Empedocles S A, Neuhauser R and Bawendi M G 1999 Three-dimensional orientation measurements of symmetric single chromophores using polarization microscopy *Nature* **399** 126–30

[21] Brokmann X, Coolen L, Dahan M and Hermier J P 2004 Measurement of the radiative and nonradiative decay rates of single CdSe nanocrystals through a controlled modification of their spontaneous emission *Phys. Rev. Lett.* **93** 107403

[22] Xiao L H, Qiao Y X, He Y and Yeung E S 2010 Three dimensional orientational imaging of nanoparticles with Darkfield microscopy *Anal. Chem.* **82** 5268–74

[23] Siyushev P *et al* 2009 Low-temperature optical characterization of a near-infrared single-photon emitter in nanodiamonds *New J. Phys.* **11** 113029

[24] Batalov A, Jacques V, Kaiser F, Siyushev P, Neumann P, Rogers L J, McMurtrie R L, Manson N B, Jelezko F and Wrachtrup J 2009 Low temperature studies of the excited-state structure of negatively charged nitrogen-vacancy color centers in diamond *Phys. Rev. Lett.* **102** 195506

[25] Englund D, Shields B, Rivoire K, Hatami F, Vuckovic J, Park H and Lukin M D 2010 Deterministic coupling of a single nitrogen vacancy center to a photonic crystal cavity *Nano Lett.* **10** 3922–6

[26] Hwang J, Pototschnig M, Lettow R, Zumofen G, Renn A, Gotzinger S and Sandoghdar V 2009 A single-molecule optical transistor *Nature* **460** 76–80

[27] Yelisseyev A P, Steeds J W, Babich Y V and Feigelson B N 2006 A new approach to investigation of nickel defect transformation in the HPHT synthetic diamonds using local optical spectroscopy *Diam. Relat. Mater.* **15** 1886–90

[28] Troupis D K, Gaudin O, Whitfield M D and Jackman R B 2002 Ion implantation of sulphur, boron and nitrogen in diamond: a charge-based deep level transient spectroscopic investigation *Diam. Relat. Mater.* **11** 342–6

[29] Shiryaev A A, Frost D J and Langenhorst F 2007 Impurity diffusion and microstructure in diamonds deformed at high pressures and temperatures *Diam. Relat. Mater.* **16** 503–11

[30] Fizgeer B, Uzan-Saguy C, Cytermann C, Richter V, Avigal I, Shaanan M, Brener R and Kalish R 2001 Inhibition of light element diffusion in diamond due to ion implantation related defects *Phys. Status Solidi* a **186** 281–9

[31] Polman A 1997 Erbium implanted thin film photonic materials *J. Appl. Phys.* **82** 1–39

[32] Favennec P N, Lharidon H, Moutonnet D, Salvi M and Gauneau M 1990 Optical activation of Er^{3+} implanted in silicon by oxygen impurities *Japan. J. Appl. Phys.* 2 **29** L524–6

[33] Michel J, Benton J L, Ferrante R F, Jacobson D C, Eaglesham D J, Fitzgerald E A, Xie Y H, Poate J M and Kimerling L C 1991 Impurity enhancement of the 1.54-MU-M Er^{3+} luminescence in silicon *J. Appl. Phys.* **70** 2672–8

[34] Gali A, Lowther J E and Deak P 2001 Defect states of substitutional oxygen in diamond *J. Phys.:Condens. Matter.* **13** 11607–13

[35] Schmidt J, Krain R, Bothe K, Pensl G and Beljakowa S 2007 Recombination activity of interstitial chromium and chromium–boron pairs in silicon *J. Appl. Phys.* **102** 123701

[36] Mishra K 1996 Identification of Cr in p-type silicon using the minority carrier lifetime measurement by the surface photovoltage method *Appl. Phys. Lett.* **68** 3281–3

[37] Zaitsev A M 2000 Vibronic spectra of impurity-related optical centers in diamond *Phys. Rev.* B **61** 12909–22

[38] Santori C, Barclay P E, Fu K M C and Beausoleil R G 2009 Vertical distribution of nitrogen-vacancy centers in diamond formed by ion implantation and annealing *Phys. Rev.* B **79** 125313

[39] Liggins S, Newton M E, Goss J P, Briddon P R and Fisher D 2010 Identification of the dinitrogen ⟨001⟩ split interstitial H1a in diamond *Phys. Rev.* B **81** 085214

[40] Pezzagna S, Naydenov B, Jelezko F, Wrachtrup J and Meijer J 2010 Creation efficiency of nitrogen-vacancy centres in diamond *New J. Phys.* **12** 065017

[41] Goss J P, Briddon P R, Rayson M J, Sque S J and Jones R 2005 Vacancy-impurity complexes and limitations for implantation doping of diamond *Phys. Rev.* B **72** 035214

[42] Fu K M C, Santori C, Barclay P E and Beausoleil R G 2010 Conversion of neutral nitrogen-vacancy centers to negatively charged nitrogen-vacancy centers through selective oxidation *Appl. Phys. Lett.* **96** 121907